ELSEVIER

International Journal of Mass Spectrometry 220 (2002) 281–288

International Journal of Mass Spectrometry

www.elsevier.com/locate/ijms

Photoionisation of ethylene clusters by synchrotron radiation in the energy range 17–50 eV

P. Franceschi [a], P. Tosi [a], D. Ascenzi [a], D. Bassi [a,*], M. Coreno [b], M. de Simone [c]

[a] INFM—Dipartimento di Fisica, Università degli Studi di Trento, I-38050 Povo, Italy
[b] INFM—Lab. TASC, I-34012 Trieste, Italy
[c] INFM—Dipartimento di Fisica, Università di Roma 3, I-00146 Rome, Italy

Received 20 November 2001; accepted 4 March 2002

Abstract

In this work, we have investigated the photoionisation of ethylene clusters in the energy range between 17 and 50 eV by following the yield of $C_3H_5^+$, $C_4H_7^+$, and $C_4H_8^+$ product ions. The formation of these stable molecular ions, by conversion into molecular bonds of the weak van der Waals bonds between the ethylene molecules, demonstrates that photoionisation can provide a mechanism for the synthesis of complex molecules from simpler units. The possible role of the ionisation of van der Waals clusters evaporated from dust grains as a complementary mechanism for the synthesis of complex organic molecules in the interstellar medium is discussed. (Int J Mass Spectrom 220 (2002) 281–288)

Keywords: Photoionisation; C_2H_4; Cluster; Synchrotron radiation

---

1. Introduction

The ionisation of ethylene clusters has been extensively studied in the past. One motivation for such studies concerns the possibility to form the loosely bound intermediate complex $C_2H_4^+ \cdot C_2H_4$ of the ethylene ion–molecule reaction [1]. The collision complex cannot be stabilised in bimolecular reactions but might be produced by photoionisation of the ethylene dimer, thus, allowing a complementary way to investigate the reactive process starting from the intermediate $[C_4H_8^+]^*$ instead of the initial reactants $C_2H_4^+ + C_2H_4$.

Lee and co-workers [1] carried out the first investigation by using a hydrogen discharge lamp to photoionise ethylene clusters in the photon energy range between 9 and 12 eV. Threshold measurements allowed them to estimate the stability of the ion–molecule collision complex to be 18.2 ± 0.5 kcal/mol. In addition to the $(C_2H_4)_2^+$ intermediate, the dissociation products $C_3H_5^+$ and $C_4H_7^+$ were also observed and it was concluded that the corresponding fragmentation processes occur via prior isomerisation into the $C_4H_8^+$ butene ion. The photoionisation of neutral ethylene dimers was reinvestigated by Ng and co-workers [2,3]. They estimated the dissociation energy of $(C_2H_4)_2^+$ to be 15.8 ± 1 kcal/mol. Baer and co-workers carried out the most recent investigation, in a narrow photon energy range around 10 eV, coupling a H_2 discharge lamp to a TOF mass spectrometer [4]. They concluded that the photoionisation of the dimer produces a stable

---

[*] Corresponding author. E-mail: bassi@science.unitn.it

PII S1387-3806(02)00685-1

$C_4H_8{}^+$ species, though its structure is not known. Above the dissociation limit, the dimer ion dissociates by first rearranging to the butene ion structure. Finally, neutral trimers are ionised purely dissociatively contributing to the $C_4H_8{}^+$ signal.

A common feature of all the experiments described above is the attempt to infer the composition of the neutral cluster beam by the analysis of mass spectra. There is no doubt that this procedure introduces some ambiguity, since significant fragmentation following the ionisation process is the general rule. At present, the only size-selected investigation of the ionisation of the ethylene dimer has been performed by Buck et al. [5]. Unfortunately, this experiment makes use of electron beam ionisation and thus, the results are not equivalent to those obtained in photoionisation measurements.

The overall picture that emerges from previous work indicates that as soon as the photon energy increases above the dissociation limit $(C_2H_4)_2{}^+$ begins to dissociate. This is consistent with recent calculations [6] of the $C_4H_8{}^+$ potential energy surface. No data are available for photon energies higher than 20 eV.

In this work, photoionisation efficiency (PIE) curves for $C_2H_4{}^+$, $C_3H_5{}^+$, $C_4H_7{}^+$, and $C_4H_8{}^+$ ions have been measured in the 17–50 eV range by using synchrotron radiation from the Gas Phase Photoemission Beam-line at Elettra, Trieste. Our experimental data extend PIE spectra already available in the literature to higher photon energies [2] and show the presence of a significant and unexpected amount of $C_4H_8{}^+$ at photon energies well above the ground state dissociation limit.

2. Experimental

The supersonic molecular beam apparatus for the Gas Phase Beam-line at Elettra was specifically designed for photoionisation experiments on atomic and molecular clusters.

For the series of experiments presented in this paper only a moderate resolving power was used ($E/\Delta E <$ 3000) and therefore, the monochromator was run in the “energy scan” mode, scanning simultaneously both the mirror and grating of the monochromator [7]. Photoionisation spectra were recorded by means of a quadrupole mass spectrometer. The use of quadrupole mass spectrometry for ionisation experiments on supersonic molecular beams is well documented [8].

The original set up of the Gas Phase branch-line [9] was modified to add differential pumping in order to decouple the UHV environment of the beam-line from the high vacuum of the experimental chamber. A brief description of the modified Gas Phase branch-line and of the Molecular Beam apparatus will is given below.

Clusters were produced by means of supersonic expansion of a 10% mixture of ethylene in argon through a 50 μm diameter nozzle. The molecular beam source operated at room temperature and at a stagnation pressure of about 1.5 bar. Under these conditions, photoionisation of the cluster beams does not yield ion products with masses higher than 56 amu ($C_4H_8{}^+$).

2.1. The molecular beam machine

The molecular beam machine consists of a single vacuum chamber, which is divided into two independently pumped sections, see Fig. 1. The source section is pumped by a 2000 L/s turbomolecular pump, while a 750 L/s turbomolecular pump evacuates the beam section. Both are backed by two separate 50 m^3/h oil-free pumps. The skimmed-supersonic molecular beam emerging from the source section proceeds into the beam section, where it is crossed at 90° by the synchrotron light beam for photoionisation. Ionic products are collected inline with the molecular beam direction by a set of optics, focused by an Einzel lens and injected along the axis of a quadrupole mass spectrometer for mass analysis and detection.

The supersonic expansion takes place in the source section, which contains a continuous molecular beam source mounted on an xyz translator in order to optimise the nozzle-skimmer distance (down to a minimum of ∼1 mm) and alignment. The source can be cooled down to ∼170 K using a liquid nitrogen cryostat mounted on one side of the vacuum chamber and connected to the nozzle by means of a copper cold

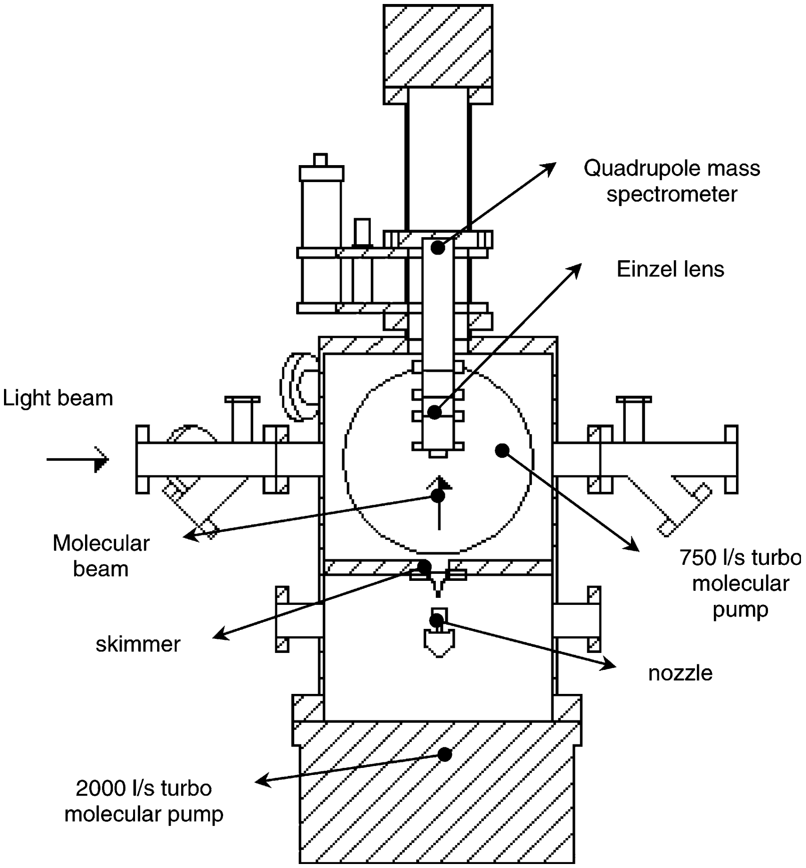

Fig. 1. Schematic view of the supersonic molecular beam apparatus.

finger. The temperature may be increased using a constantan heating wire wound around the nozzle. A thermocouple is mounted on the nozzle tip for an accurate monitor of the nozzle temperature.

A fixed skimmer (Beam Dynamics Inc. model 2, $\varnothing = 0.42\,\text{mm}$) for collimation of the supersonic expansion separates the source section from the beam section. A mechanical chopper is mounted in the beam path, a few centimetres away from the skimmer, to modulate the molecular beam in order to allow for subtraction of the background signal from that of the molecular beam. The chopper is driven by a high-vacuum compatible stepper motor (Model B14.1 with SMD1 driver from Arun Microelectronics Ltd.). The interaction region between the molecular beam and the synchrotron radiation is about 10 cm from the skimmer and its size is determined by the dimensions of the molecular and light beams (the latter being $3\,\text{mm} \times 1\,\text{mm}$). The ion optics for extraction of the products are mounted on-axis along the molecular flight direction. An electrostatic Einzel lens focuses the ion beam into the quadrupole. An additional electron impact ion source is used to check the system efficiency when synchrotron radiation is not available. After mass selection, ions are deflected at 90° by an electrostatic system, and are then detected by a Channeltron electron multiplier. The data acquisition is fully managed by a personal computer running a LabVIEW (National Instruments©) control program, which also drives the stepper motor motion.

2.2. The modified Gas Phase branch-line

The original optical design of the Gas Phase branch-line was intended for experiments with a full field imaging microscope [9] and it consisted of two optical elements.

A toroidal mirror could be inserted into a vacuum chamber placed after the exit slit of the monochromator and was used to deflect the light 12° to the left of the Gas Phase main line light path. The deflection mirror manipulator provides linear movements in a horizontal direction to insert or remove the mirror, as well as pitch, roll and yaw movements for alignment of the light onto a second toroidal mirror that was attached to the microscope vacuum chamber and was used to steer the light onto the sample. Between the two mirrors, at the focus of the deflection mirror, a diagnostic chamber was equipped with a fluorescent screen and a calibrated photodiode type AXUV-100, which could be inserted to measure the photon flux.

In the current set-up for gas phase experiments only the first toroidal deflection mirror has been retained, providing a horizontal magnification of 3.4 and a vertical magnification of 4.4. At the diagnostic chamber, 3 m away from the toroidal mirror, we obtain an elliptical spot of approximately 0.4 and 1.5 mm FWHM in the vertical and horizontal directions, respectively. Experimental chambers can be placed after the diagnostic chamber that has also been provided with a 280 L/s turbomolecular pump in order to constitute the first of four differential pumping sections between the end-station and the deflection mirror chamber. The remaining sections are obtained by a sequence of three diaphragms plus ion pump units, mounted on a single frame having the light path at its centre and approximately 50 cm in length along the beam path. The diaphragms are rectangular, 2 mm × 4 mm (vertical × horizontal) and are 6 mm thick, and the ion pumps are 40 L/s Varian Starcell pumps. The complete differential pumping system can maintain a pressure ratio up to 20,000 between the experimental chamber and the deflection chamber. The highest pressure allowed in the beam diagnostic chamber is set at 1×10^{-4} mbar by the beam-line vacuum control system. If higher pressure drops are needed between the experimental end station and the deflection chamber additional diaphragms can be mounted at the CF-35 exit port of the diagnostic chamber.

A windowless photoionisation gas cell can be placed after the experimental station. It is equipped with a photodiode and allows calibration of the photon energy scale and measurement of the incident flux.

3. Results and discussion

All the photoionisation efficiency curves have been normalised to the incident photon flux. Higher order contributions to the signal have also been taken into account as these are a notorious problem in the low energy range (17–40 eV) for grazing incidence wide energy range beam-lines. For the normalisation of the data we used the first order light photocurrent yield of the photodiode. In the 17–22 eV photon energy range, it was obtained by filtering through He at 10 mbar to remove higher order photons. Solid states transmission filters (Mg and Al) were used for more energetic photons.

The $C_2H_4^+$ PIE spectrum shown in Fig. 2 extends previous results [2,10] to higher energies. Thanks to the higher spectral resolution, our spectra show a richer structure. The precise assignment of the new peaks would require the scan in energy to be made using smaller steps, and has been postponed to future investigations.

In addition to the monomer signal, we detect many different ion clusters. As already discussed, a general difficulty arises when trying to relate the observed ion distribution to the neutral cluster composition of the molecular beam. A common approach to the problem is to control the neutral cluster population by varying the expansion conditions. As an example, the expansion setting that maximises the production of ethylene dimers is established by searching for those conditions for which ions containing more than four carbon atoms are not observed [1,2]. Unfortunately this procedure does not exclude the possibility that these ions may result from fragmentation of large neutral clusters.

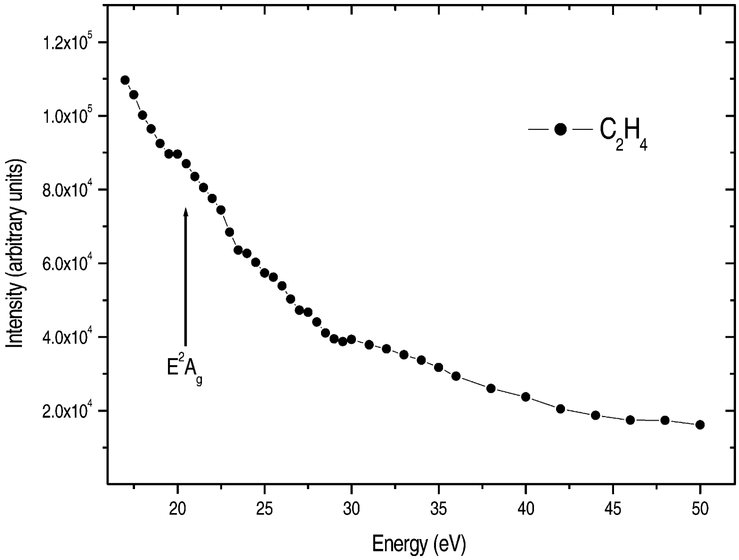

Fig. 2. Photoionisation efficiency (PIE) curve for $C_2H_4^+$ in the 17–50 eV energy range.

In a different approach, Baer and co-workers [4] studied the shape of TOF peaks as a function of expansion conditions. The underlying idea is that ions resulting from a fragmentation process should have broader TOF peaks due to the kinetic energy release following the fragmentation. In fact, they observed that the $C_4H_8^+$ peak is composed of two contributions: a narrow peak attributed to the direct ionisation of the dimer, and a broader peak that results from the dissociative ionisation of larger clusters. Thus, the partial suppression of the last contribution is supposed to coincide with an increase of the relative population of dimers in the neutral beam.

As already mentioned, the only mass selected ethylene cluster experiment to have been reported was performed by Buck et al. [5]. They used a He beam to scatter specific cluster sizes at different angles. Mass spectra obtained using 100 eV electrons were collected for different $(C_2H_4)_n$ neutral clusters ($2 < n < 7$). A striking difference from photoionisation experiments is the lack of the dimer ion signal, since the latter results only from the ionisation of larger clusters. In addition, the dissociative ionisation of trimers by electrons does not produce ions larger than $C_4H_8^+$. It is worth pointing out that results from electron bombardment ionisation are not directly comparable with photoionisation data, however, we tentatively argue that the fragmentation observed when using electrons establishes the upper limit for the photoionisation process at the same energy. Following this hypothesis, the absence of ionic products heavier than $C_4H_8^+$ implies that our cluster beam is mainly composed of neutral dimers, possibly some trimers, and a much lower amount of heavier clusters.

The photoionisation efficiency curves for $C_3H_5^+$, $C_4H_7^+$, and $C_4H_8^+$ are shown in Fig. 3. In agreement with previous investigations, the most abundant fragment is $C_3H_5^+$. This fact has been rationalised on the basis of a statistical model that predicts the relative abundance of the products as a function of both energy and angular momentum in the dissociating $C_4H_8^+$ ion [11]. The main difference between our results and those of previous experiments is that we detect a relatively large amount of $C_4H_8^+$ ions, although at different photon energies. Baer and co-workers [4] in a threshold photoelectron–photoion coincidence (TPEPICO) experiment have clearly shown that for photon energies above the first dissociation limit (about 10.30 eV), ions produced by ionisation of neutral dimers rearrange into the butene ion structure and

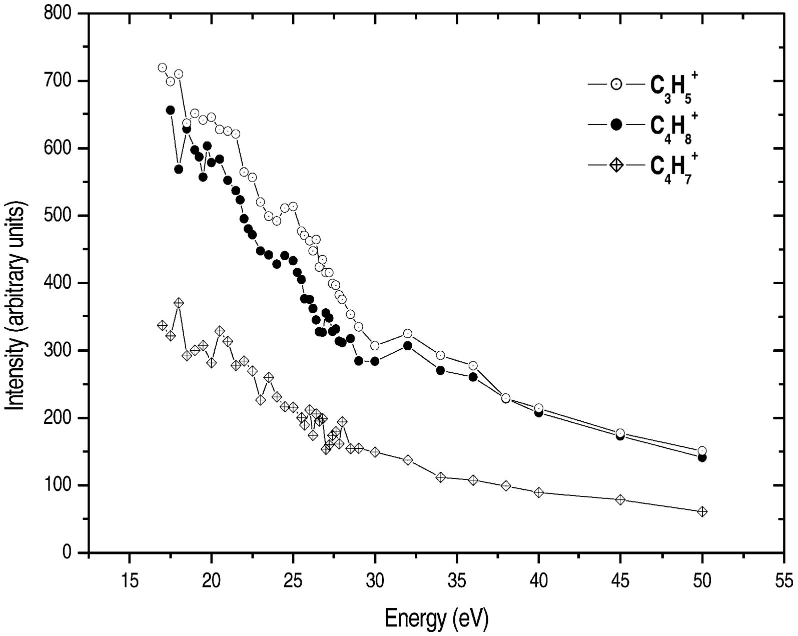

Fig. 3. Photoionisation efficiency (PIE) curves for $C_3H_5^+$, $C_4H_7^+$, and $C_4H_8^+$ in the 17–50 eV energy range.

then dissociate. The PIE study reported here is not an energy-selected experiment, and therefore $C_4H_8^+$ ions could be formed at high photon energies because of the photoelectron can carry kinetic energy. However, previous non-energy-selected works [2] have shown that by increasing the photon energies above the dissociation limit of $C_4H_8^+$ ion, the production of this specie decreases dramatically with respect to that of the fragments. Thus, our observation of $C_4H_8^+$ at much higher photon energies (between 17 and 50 eV) may be explained by assuming that either (a) $C_4H_8^+$ originates by dissociative photoionisation of trimers and heavier clusters, or (b) in our energy range $C_4H_8^+$ ions are produced in excited states, not accessible at lower photon energies, whose lifetimes are longer than the time scale of our experiment. Hypothesis (a) seems to be contrary to the observation that mass 56, i.e. $C_4H_8^+$, is the largest mass detected in our experiment. If the neutral beam were to contain a large fraction of trimers and higher order clusters, then additional peaks corresponding to mass 69 ($C_5H_9^+$) and larger ones should also be detected [3,4]. On the other hand, we have no independent measurements to support hypothesis (b). Further experiments, making use of the Buck's method for mass selecting neutral clusters, would be necessary to clarify this possibility.

Concerning the energy dependence of the PIE spectra, it is interesting to note the overall resemblance between the $C_4H_8^+$, $C_4H_7^+$, $C_3H_5^+$ PIE curves and that for $C_2H_4^+$. Deeper understanding of the possible correspondences needs better energy resolution and the complete assignment of the structures observed in the monomer spectrum.

The photoionisation of dimers has often been interpreted in terms of ionisation of a single ethylene unit within the cluster. In this picture, $C_3H_5^+$ and $C_4H_7^+$ are formed in the intra-cluster ion–molecule reaction $C_2H_4^+ + C_2H_4$ [1,5], while $C_4H_8^+$ should not be observed [5]. However, the above mechanism is legitimate only if the interaction in the ionic dimer does not differ too much from that in the neutral dimer. This assumption is generally dubious because of the bond stabilisation due to the charge transfer coupling [12], which causes the mixing of the electronic states of the separate reactants. Furthermore, the notion that the ionisation of a van der Waals dimer involves only one unit is true only for a direct process, but not for autoionisation of excited states, since in this case the ejected electron experiences the whole dimer field. A more realistic picture should consider the formation of an excited $[C_4H_8{}^+]^*$ species, whose later fate depends on the details of the potential energy surface [4,6]: the nascent $[C_4H_8{}^+]^*$ ion may either be stabilised into a bound state or dissociate into the observed fragments [13].

The formation of $C_4H_8{}^+$ following the photoionisation of $(C_2H_4)_2$ is particularly interesting as it is a further demonstration of the possibility to synthesise complex molecules starting from simple building blocks within van der Waals clusters. This process has been previously explained in terms of intracluster reactions [13–16]. Whatever the explanation, van der Waals clusters can be transformed into stable molecules either via intracluster reactions initiated by ionisation or by the ionisation process itself. This should be true whenever the ion is a chemically bound species: beside the system discussed in the present work, another clear example is the production of $N_4{}^+$ starting from $(N_2)_2$, in which the neutral dimer is weakly bonded but the bonding in the ion is about 1 eV [17]. In contrast to any naive expectations, energetic radiation instead of breaking the weak van der Waals bond may convert it into a strong one, a point whose practical importance might have been underestimated. This process is possibly relevant to the synthesis of complex organic molecules detected in interstellar space. Mechanisms based on gas-phase reactions explain the production of simple compounds, but cannot describe how complex chemicals are formed in significant amounts. It is now believed that molecules could form on dust grains in the interstellar clouds. Recently, Bernstein et al. [18] have demonstrated that the UV photolysis of polycyclic aromatic hydrocarbons (PAHs) in water ice produces complex molecules, such as alcohols, quinones and ethers. Thus, they suggested that the photochemistry of PAHs in the condensed phase might be an important source of interstellar organic molecules. One problem is that the newly formed molecules would remain trapped on the ice, and the energy necessary to desorb the molecules would also be strong enough to break them. We tentatively suggest here a complementary mechanism that overcomes the problem. Solid materials irradiated by energetic radiation or particles liberate molecules and atoms, either ionised or neutral, and also large amounts of droplets and clusters [19,20]. Thus, it is imaginable that clusters desorbed from the grain surface might be present in the gas phase and that their successive ionisation results in the production of complex molecules as discussed in this paper.

Acknowledgements

The authors are grateful to Dr. K.C. Prince for helpful discussions and suggestions. They also thank A. Rossi, L. Romanzin, M. Sieff and G. Silvestrin who contributed in different periods to the development of the experimental apparatus. Pietro Franceschi acknowledges support from INFM under the Synchrotron Radiation grant program.

References

[1] S.T. Ceyer, P.W. Tiedemann, C.Y. Ng, B.H. Mahan, Y.T. Lee, J. Chem. Phys. 70 (1979) 2138.
[2] Y. Ono, S.H. Linn, W.B. Tzeng, C.Y. Ng, J. Chem. Phys. 80 (1984) 1482.
[3] W.B. Tzeng, Y. Ono, S.H. Linn, C.Y. Ng, J. Chem. Phys. 83 (1985) 2813.
[4] J.A. Booze, T.N. Feinberg, J.W. Keister, T. Baer, J. Chem. Phys. 100 (1994) 4294.
[5] U. Buck, C. Lauenstein, H. Meyer, R. Sroka, J. Chem. Phys. 92 (1988) 1916.
[6] P. Jungwirth, T. Bally, J. Am. Chem. Soc. 115 (1993) 5783.
[7] K.C. Prince, R.R. Blyth, R. Delanuay, M. Zitnik, J. Krempasky, J. Slezak, R. Camilloni, L. Avaldi, M. Coreno, G. Stefani, C. Furlani, M. De Simone, S. Stranges, J. Synchrotron Radiat. 5 (1998) 565.
[8] C.Y. Ng, Vacuum Ultraviolet Photoionization and Photodissociation of Molecules and Clusters, World Scientific, Singapore, 1991.
[9] T. Schmidt, J. Slezak, S. Heun, R.R. Blyth, R. Delanuay, D. Cocco, K.C. Prince, E. Bauer, M. Coreno, J. Synchrotron Radiat. 6 (1999) 957.
[10] D.M. Holland, D.A. Shaw, M.A. Hayes, L.G. Shpinkova, E.E. Rennie, L. Karlsson, P. Baltzer, B. Wannberg, Chem. Phys. 219 (1997) 91.

[11] W.J. Chesnavich, L. Bass, T. Su, M.T. Bowers, J. Chem. Phys. 74 (1981) 2228.

[12] F. Pirani, A. Giulivi, D. Cappelletti, V. Aquilanti, Mol. Phys. 98 (2000) 1749.

[13] Q. Zhong, L. Poth, Z. Shi, J.V. Ford, A.W. Castleman Jr., J. Phys. Chem. B 101 (1997) 4202.

[14] M.T. Coolbaugh, W.R. Peifer, J.F. Garvey, Chem. Phys. Lett. 168 (1990) 337.

[15] M.T. Coolbaugh, G. Vaidyanathan, W.R. Peifer, J.F. Garvey, J. Phys. Chem. 95 (1991) 8337.

[16] S.G. Whitney, M.T. Coolbaugh, G. Vaidyanathan, J.F. Garvey, J. Phys. Chem. 95 (1991) 9625.

[17] P. Tosi, W. Lu, D. Bassi, R. Tarroni, J. Chem. Phys. 114 (2001) 2149.

[18] M.P. Bernstein, S.A. Sandford, L.J. Allamandola, J.S. Gillette, S.J. Clemett, R.N. Zare, Science 283 (1999) 1135.

[19] R. Kelly, A. Miotello, Nucl. Instr. Meth. Phys. Res. B 122 (1997) 374.

[20] L.E. Rehn, R.C. Birtcher, S.E. Donnelly, P.M. Baldo, L. Funk, Phys. Rev. Lett. 87 (2001) 207601.